Sādhanā Vol. 27, Part 4, August 2002, pp. 425–448. © Printed in India

Embrittlement and decrease of apparent strength in large-sized concrete structures

ALBERTO CARPINTERI and BERNARDINO CHIAIA

Department of Structural Engineering, Politecnico di Torino, Corso Duca degli Abruzzi 24, 10129 Torino, Italy
e-mail: {carpinteri, chiaia}@polito.it

Abstract. The problem of scale-effects on the performances of concrete structures is discussed. Experimentally observed decrease of nominal tensile strength, accompanied by structural embrittlement, occurring in large structures is of crucial importance in modern concrete engineering. Most of the previous approaches to the problem are restricted to notched structures and they often fail to predict mechanical behaviour in real situations. The physical approach put forward by us takes into adequate account the effects of microstructural disorder and seems to be valid in the whole size range, at least for unnotched structures. Thereby, reliable predictions can be made of the material properties in large-sized concrete structures.

Keywords. Concrete structures; size-effects; fractal geometry.

1. Introduction

The problem of scaling is of central importance in any physical theory. In the field of structural mechanics, the study of scale-effects is acquiring a prominent role, due to the need for proper prediction of the mechanical properties in large-sized structures, starting from the available test data. The development of high-performance materials, coupled with more restrictive safety rules, also requires a more precise knowledge of the structural behaviour of large-sized structures.

In solid mechanics, a distinction has to be made between the structural (intrinsic) scale-effects and *nominal* size effects on the apparent mechanical quantities. Regarding the first effect, the transition from ductile to brittle behaviour can be evidenced when the size of the structure increases (Carpinteri 1986). This kind of scale-effect is detected in all engineering materials (e.g., the brittleness of Liberty ships as compared to the ductility of Griffith's glass filaments). As the size of a structure increases, a more catastrophic failure is expected because the rate of energy release due to fracture is progressively higher than the rate of energy consumption on the crack surface. Dimensional analysis is perhaps the best tool to get a first physical insight into this phenomenon. While, in fact, the energy release rate scales with the structure size according to $[L]^3$, the energy dissipated on the crack surface scales according only to $[L]^2$. Carpinteri & Chiaia (1996) have demonstrated that this dimensional competition is smoothed when energy dissipation occurs also in the volume, as it is the case of process zones where damage and plasticity

occur, or when it takes place within fractal domains with dimension larger than 2.0 (intermediate sets between surfaces and volumes). In all these cases, a more ductile collapse occurs.

The most important scale effect on nominal material properties is the effect of structure size on apparent strength (Bažant & Chen 1997). This problem was initially addressed by Leonardo da Vinci, who can be considered the first theorist of the so-called statistical size-effect. He stated, in fact, that "*if two ropes have the same thickness, the longest is the weakest*". Later, but still two centuries before the development of the modern probability theory, the French scientist E Mariotte observed the random scatter of material properties and shed new light onto material science. However, the modern statistical approach is based on the weakest link concept, originally proposed by Weibull (1939) and later developed by Freudenthal (1968) and Carpinteri (1986) among others. In this context, the size effect on nominal strength is provided by the probability of meeting the most critical defect (depending on its size and orientation), which obviously increases with increase in structural size.

A more systematic discussion on the problem can be found in the well-known book by Galileo (Galilei 1638). Starting from the observation of nature, Galileo concluded that, if the skeletons of small and large vertebrates are compared, a transition from slender to thick bones is observed (figure 1). The bones increase more than proportionally to the linear size of the animal, because of the interplay of the animal weight ($\sim [L]^3$) and of the bone strength ($\sim [L]^2$). Nowadays we know that the contribution of the skeleton to the total weight in vertebrates is percentually higher in large animals, representing only 8% for mice, 14% for dogs, 18% for humans and 27% for elephants (D'Arcy 1917). It is interesting to note that the above conclusion holds only in the case of terrestrial vertebrates. In fact, if the shapes (and the skeletons) of a whale and of a dolphin are compared, it seems that a perfect structural similitude is maintained. Recalling dimensional analysis, one can easily conclude that this is due to the hydrostatic thrust ($\sim [L]^3$) which counterbalances the gravitational force.

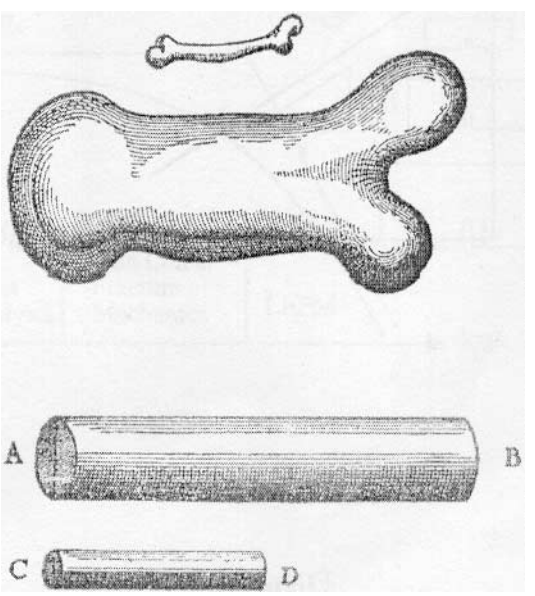

Figure 1. Original drawings on size-effects by Galileo.

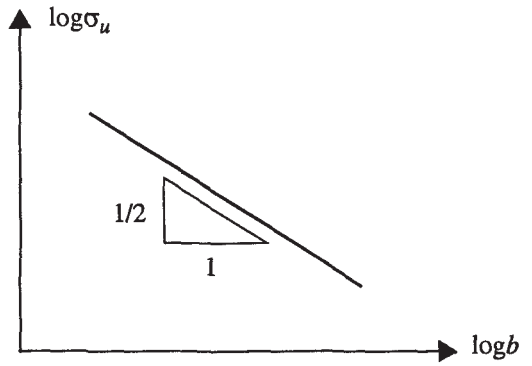

Figure 2. Size effect on strength according to LEFM.

Moving to modern times, a major advance was made by Griffith (1921). Its well-known energy-based approach for crack propagation naturally provides that the nominal strength σ_u decreases with the structural size b according to:

$$\sigma_u \sim b^{-1/2}. \tag{1}$$

If the Irwin's stress approach (Irwin 1957) is adopted, the same scaling behaviour is obtained by simply applying dimensional analysis to the usual parameters governing Linear Elastic Fracture Mechanics (LEFM). In fact, the dimensional disparity between tensile stress $\sigma([\mathrm{F}][\mathrm{L}]^{-2})$ and stress-intensity factor $K_I([\mathrm{F}][\mathrm{L}]^{-3/2})$ causes a constant slope equal to $-1/2$ in the nominal strength vs. structural size bilogarithmic diagram, as shown in figure 2 (Carpinteri 1989). It has been shown (Carpinteri 1994b) that this corresponds to a limit condition of extreme disorder, and cannot be considered universal behaviour valid for the whole size range of unnotched structures. Only when the size of the crack is sufficiently large, will the LEFM singularity play a pre-eminent role. Also, if the smooth cracks are substituted by fractal cracks (Carpinteri & Chiaia 1996), which are clearly a better approximation to reality, the stress singularity power exponent decreases yielding a slope smaller than $-1/2$ in the log-log plot.

In 1984, Bažant proposed the so-called Size Effect Law for concrete (SEL), where LEFM and limit analysis concepts were joined together yielding:

$$\sigma_u = B f_t / \left[1 + (b/b_0)\right]^{1/2}, \tag{2}$$

where f_t is the plastic limit stress, B and b_0 are two constants to be determined in each case by fitting the experimental data (figure 3).

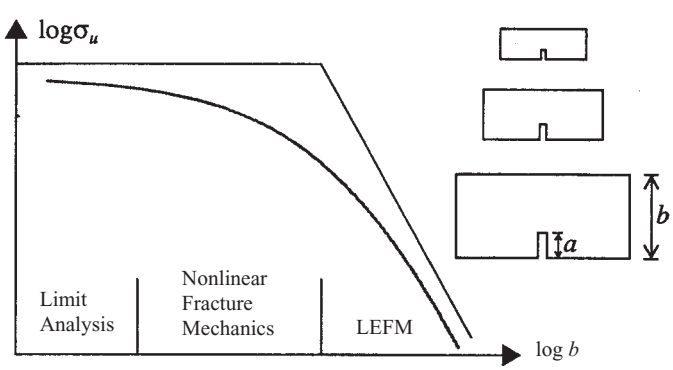

Figure 3. Bažant's size effect law (SEL).

As shown in figure 3, in order to derive (2), bažant assumed that the total potential energy, released during fracture, is proportional to the square of the crack length a, which scales proportionally to the specimen size b (i.e., $a/b =$ constant). At the same time, the energy dissipation is proportional to a, because the width of the crack band is assumed to be constant and proportional to the maximum aggregate size ($nd_{\max}$). Several analyses on the notch sensitivity behaviour using the fictitious crack model by Hillerborg *et al* (1976) have supported Bažant's SEL and, because scaling effects are present even in members without initial cracks, the SEL was erroneously extended also to unnotched geometries.

Several experimental results, however, indicate that even the largest members without initial crack resist some stress, contrary to the SEL predictions. Therefore, based on this experimental evidence, some theoretical explanations of the inadequacy of (2) have been provided in the recent literature. Bruhwiler *et al* (1991) argued that the effect of $d_{\max}$ on the scaling behaviour of concrete is not consistent with that predicted by SEL. Tang *et al* (1992) pointed out the essential misunderstanding in the hypotheses on which SEL is based. Bažant obtained his formulation only for notched specimens and assumed that the notch size a, responsible for the stress singularity, was scaled proportional to the structural size. When applying the SEL to unnotched specimens, the above hypothesis falls because in real disordered materials the size a of the characteristic flaw, which is responsible for the crack propagation, is independent of the specimen size. This clear disagreement from reality causes the anomalous behaviour of Bažant's SEL, which, in the limit of infinite structural size, incorrectly results in being totally governed by Linear Elastic Fracture Mechanics. In this way, one should expect a (unrealistic) value of tensile strength equal to zero for very large structures (figure 3).

Some attempts have been made to put into the model the variable influence of the characteristic flaw size a, in the case of initially unnotched specimens. An empirical Modified Size Effect Law (MSEL) was proposed by Kim & Eo (1990), in order to fit the experimental data obtained from Brazilian splitting tests on concrete cylinders (Hasegawa *et al* 1985), where the inadequacy of SEL was strongly evidenced (see figure 13 in § 4). The MSEL equation was obtained by simply adding a constant corrective parameter to Bažant's equation:

$$\sigma_u = \left\{ B f_t / [1 + (b/b_0)]^{1/2} \right\} + \alpha f_t. \tag{3}$$

By applying the MSEL, a more realistic asymptotic non-zero value of the tensile strength can be determined, in the limit of infinite structural sizes. However, (3) depends on three-parameters, and Planas *et al* (1995) showed that the values of α, obtained by best-fitting of the experimental data, are close to 0.15, implying that too low an asymptotic value of the strength is predicted ($\sigma_u = 0.15 f_t$).

2. Size effects on the bending strength

It is nowadays widely believed that the true fracture properties of concrete structures can be unequivocally determined only by means of uniaxial tensile tests. Unfortunately, tensile tests are difficult to carry out in standard laboratories, either with fixed or rotating boundary conditions. Therefore, the ultimate bending strength, also called the *modulus of rupture* σ_u^{flex},which is measured for beams in either three-or four-point bending, turns out to be an experimentally convenient measure of strength owing to the relative simplicity of these tests. On the other hand, the strong size-dependence of the bending properties (not only of the nominal strength, but also of the rotational capacity and ductility) has been earlier detected in several investigations carried out on plain and reinforced concrete members (Neville 1981).

Indeed, the correct determination of the bending strength of real-sized structures is crucial from engineering viewpoints, due to the large amount of concrete members subjected to flexure and to the wide diffusion of bending tests throughout the laboratories. This explains the theoretical and experimental efforts made by the scientific and engineering community in order to interpret the phenomenon of the size-dependence of σ_u^{flex}, whereas only in the last ten years attention has been drawn also to the other structural geometries.

It is important to point out that uncertainties in the determination of the bending strength affect both allowable stress design and limit state design, in the former case by lowering the reliability of the safety factor and in the latter case by providing unacceptable stress–strain conditions under service loads. In both cases, exceeding prudence due to uncertainty may lead to coarse oversizing or to overestimations of the reinforcement ratios. Problems arise not only in the case of plain concrete structures (large foundation beams or massive walls) but also in reinforced members, where cracking of the most stressed concrete layers leads to corrosion of the steel bars and dramatically infers durability. Moreover, the minimum reinforcement requirements for beams subjected to bending are strongly related to the modulus of rupture. In fact, it has become clear that, especially for deep beams, the correct minimum reinforcement ratio can be computed only by means of a fracture mechanics approach (Carpinteri *et al* 1997).

Building codes usually relate the (nominal) bending strength σ_u^{flex} to a constant quantity f_{ct}, which is intended as the uniaxial tensile strength. According to the elastic bending theory, if M_u is the ultimate bending moment in the central cross section of the beam (subjected to either three-or four-point bending), and t and b are respectively the thickness and the depth of the beam, the nominal bending strength is given by:

$$\sigma_u^{flex} = 6M_u/b^2t. \tag{4}$$

If we assume that f_{ct} is the limit tensile stress that the material can locally undergo, it follows that the bending strength σ_u^{flex} coincides with f_{ct} in the case of an elastic-perfectly brittle material (figure 4a). No size-effect is provided in this case (figure 4c). In fact, catastrophic failure is supposed to occur as soon as f_{ct} is reached in any point of the beam (figure 4b). Nevertheless, this would be true in the (ideal) case of pure bending while, in the case of three-point bending, the modulus of rupture σ_u^{flex} exceeds f_{ct} by almost 5% due to the asymmetrical stress field.

A trivial relation between the modulus of rupture σ_u^{flex} and f_{ct} is provided by the ACI (1992), which merely assumes, on the average:

$$\sigma_u^{flex} = 1.25 f_{ct}. \tag{5}$$

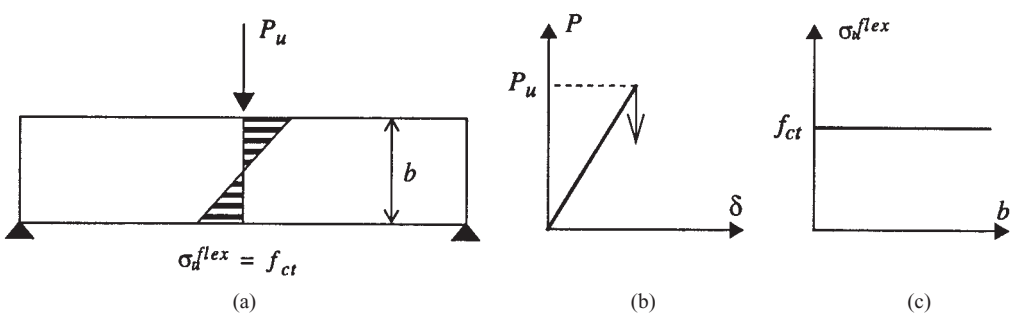

Figure 4. Elastic-perfectly brittle bending model.

The size-dependence of the bending strength is therefore not taken into account by (5), which only states that σ_u^{flex} is larger than f_{ct}, as it had been reported much earlier (Neville 1981). An analogous approach is maintained by the CEC (1994), where the concrete tensile strength f_{ct}, if measured by means of flexural tests, has to be drastically reduced by 50%:

$$\sigma_u^{flex} = 2.0 f_{ct}. \tag{6}$$

If plasticity is supposed to occur in the most stressed layers of the beam, the nominal flexural strength σ_u^{flex}, computed according to (4), is found to depend upon the strain gradient (figure 5). Shallower beams (figure 5b) do therefore yield higher values of the nominal bending strength, according to the larger strain decrease with respect to the depth (steep gradient). On the basis of this theory and of early experimental results, an empirical expression was proposed by Heilmann (1976), relating the nominal flexural strength σ_u^{flex} to the depth a of the tensile zone (figure 5a), which can be considered approximately proportional to the total beam depth b:

$$\sigma_u^{flex} = (0.8 + 0.26a^{-0.6}) f_{ct}, \tag{7}$$

where a has to be measured in metres. Note that, according to (7), the nominal bending strength σ_u^{flex} of very deep beams ($a > 1500$ mm) may become smaller than f_{ct}. Note also that these arguments would imply that the nominal bending strength increases if applied compression loads act upon the beam, thus reducing the size a of the tensile zone.

Based on a similar strain-gradient approach, a size-dependent empirical relationship between the modulus of rupture and the tensile strength has been specified in the CEB-FIP (1991) Model Code and is given by:

$$\sigma_u^{flex} = f_{ct} \left[\frac{1 + 2.0(b/b_0)^{0.7}}{2.0(b/b_0)^{0.7}} \right], \tag{8}$$

where b is the beam depth and b_0 is a reference size equal to 100 mm. Equation (8) is applicable to unnotched beams with $b \geq 50$ mm. Note that the above equation comes from experimental

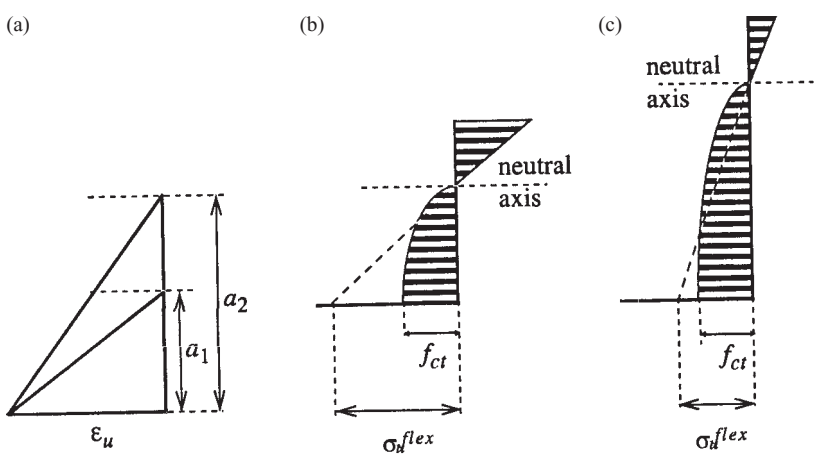

Figure 5. Effect of variable strain gradients on nominal bending strength. Shallow **(b)** vs. deep **(c)** beams.

observations and no considerations are involved regarding the role of the microstructure, whereas aggregate interlocking is explicitly taken into account in the aforementioned codes when dealing with the ultimate shear strength.

If the elastic-perfectly brittle constitutive model is abandoned, and the Cohesive Crack Model (Hillerborg *et al* 1976) is assumed to represent the mesoscopic mechanical behaviour of concrete, the size-dependence of the modulus of rupture can be more adequately described. Indeed, a unique relationship cannot be deduced, since solutions may appreciably differ from one another, depending on the shape of the softening curve (Planas *et al* 1995). Different failure mechanisms may take place, depending on the rate of consumption of the fracture energy $\mathcal{G}_F$. Nevertheless, the asymptotic behaviour predicted by the cohesive approach is $\mathcal{G}_F$-independent, and yields the following relations:

$$\sigma_u^{flex} \to 3 f_{ct} \text{ for } b \to 0, \tag{9a}$$

$$\sigma_u^{flex} \to f_{ct} \text{ for } b \to \infty, \tag{9b}$$

where the limit (9a) for structural sizes tending to zero represents a plastic limit solution, as it was shown by Carpinteri (1986).

Primary importance has been given by the Japanese scientific community to the size effect on bending strength. Among the various proposed solutions, it is worth mentioning the empirical equation put forward by Uchida (1992):

$$\sigma_u^{flex} = f_{ct} \left[1 + \frac{1}{0.85 + 4.5(b/l_H)} \right], \tag{10}$$

where $l_H = E\mathcal{G}_F/f_{ct}^2$ is the Hillerborg's characteristic length (Hillerborg *et al* 1976) and $b/l_H \geq 0.1$. For a typical concrete $l_H \approx 300$ mm whereas, in the case of high-strength mixtures, this value can eventually be halved.

The aforementioned empirical models fit the experimental results only in a narrow size range, due to the lack of theoretical bases. Moreover, appreciable differences arise between the curves, either in the case of the smaller or, which is more important, in the case of the larger beam sizes (Carpinteri *et al* 1997). However, Bažant's Size Effect Law, (2), although based on theoretical arguments, failed to interpret various three-point bending and four-point bending tests on unnotched beams (see § 4). Other nonlinear fracture mechanics models have been recently developed to explain the size-dependence of the modulus of rupture σ_u^{flex}, but they work only in a limited range. This is the case of the boundary layer model by Bažant & Li (1995) and of the two-parameter model by Jenq & Shah (1985). The former model gives an interpretation of size-effect which is alternative to SEL, and is supposed to hold when macrocracking is not occurring and energy release is not primarily involved in the definition of the peak-load. In the case of the latter model, astonishingly, the modulus of rupture seems to increase with the depth of the beam in the smaller sizes range, which represents a clear inconsistency.

In conclusion, a completely different approach should be pursued and a more general interpretation of scaling should be provided. Scale-effects have been detected in all the testing geometries and loading schemes. Thus, not only should bending size-effects be explained, but a physical model capable of interpreting all the particular situations should be put forward. Fractal geometry, coupled with the theory of critical phenomena, gives the means for developing such a non-conventional model.

3. The multifractal scaling law

3.1 *Fractal modelling of disordered materials*

It is nowadays established that the process of fracture in brittle and quasi-brittle materials should be set in the framework of critical phenomena, and should be considered a *cooperative phenomenon* with interactions at all the length scales. Moreover, experimental evidence of fractality (self-similar morphologies with non-integer physical dimensions) has been detected in the microstructure of many heterogeneous materials. Networks of surface cracks, Fracture surfaces of concrete, rocks, ceramics and metals, and Distributions of microcracks in the bulk of a stressed body possess fractal properties in a well-defined scale range. Only by an adequate modelling of the disordered microstructure, can the scaling behaviour of the mechanical quantities be consistently explained.

Carpinteri (1994a) demonstrated that the non-integer dimensions of the domains on which the physical quantities are defined assume deep significance with respect to the scaling behaviour of the same quantities. In this respect, a fundamental distinction among fractal domains has to be pointed out. The *invasive* or *densifying* fractals, i.e., the spatial sets whose Hausdorff dimension Δ is strictly larger than their topological dimension, produce positive scaling of the quantities (e.g. the fracture energy $\mathcal{G}_F$) defined over them. In the case of brittle fracture, figure 6a gives an example of an invasive fractal set ($\Delta = 2.30$), which is well-suited for modelling of the energy dissipation domain, conventionally defined as a fracture "surface" (Carpinteri & Chiaia 1995).

On the contrary, *lacunar* or *rarefying* fractals like the Sierpinski carpet (figure 6b) possess Hausdorff dimension lower than that of the domain where they are contained ($\Delta = 1.89$), and therefore provide negative scaling of the quantities (e.g. the tensile strength σ_u) defined over them. The rarefied (damaged) ligament of a heterogeneous solid subjected to tensile loading can be consistently modelled by means of this kind of fractal sets. The fundamental difference between invasive and lacunar fractals is represented by the asymptotic behaviour of the euclidean measure of the set. While, in fact, the area of an invasive fractal surface tends to infinity as the scale of observation is refined, the area of a lacunar set tends to zero. With reference to figure 6, finite measures of the fractal domains can be obtained only by means of non-integer dimensions ($[L]^{2.30}$ in the first case and $[L]^{1.89}$ in the second case.

By applying a renormalization group procedure, Carpinteri (1994a) demonstrated that, if the ligament of a stressed solid is supposed to be a self-similar lacunar set with dimension $\Delta < 2$, the nominal strength σ_u defined over this ligament scales with the linear dimension by following a power law with exponent equal to $(2 - \Delta)$. Since physical plausibility imposes a limit on the scale rarefaction rate, Δ is larger than 1.50 for most engineering materials. Thus, the decrease of strength with size is less rapid than in the case of LEFM (figure 7).

3.2 *Homogenization for infinite sizes*

The depicted self-similar (monofractal) scaling of σ_u (figure 7) is valid only within a narrow range of sizes, where the fractal dimension can be considered constant. Topological multifractality implies progressive vanishing of fractality as the scale increases. Since the microstructure of a disordered material is the same and is independent of the macroscopic size, the influence of disorder on the mechanical properties essentially depends on the interplay between an intrinsic characteristic length l_{ch} and the external size b of the specimen. Therefore, the effect of microstructural disorder on the mechanical behaviour of materials becomes progressively less important at the largest scales, whereas it represents a fundamental feature

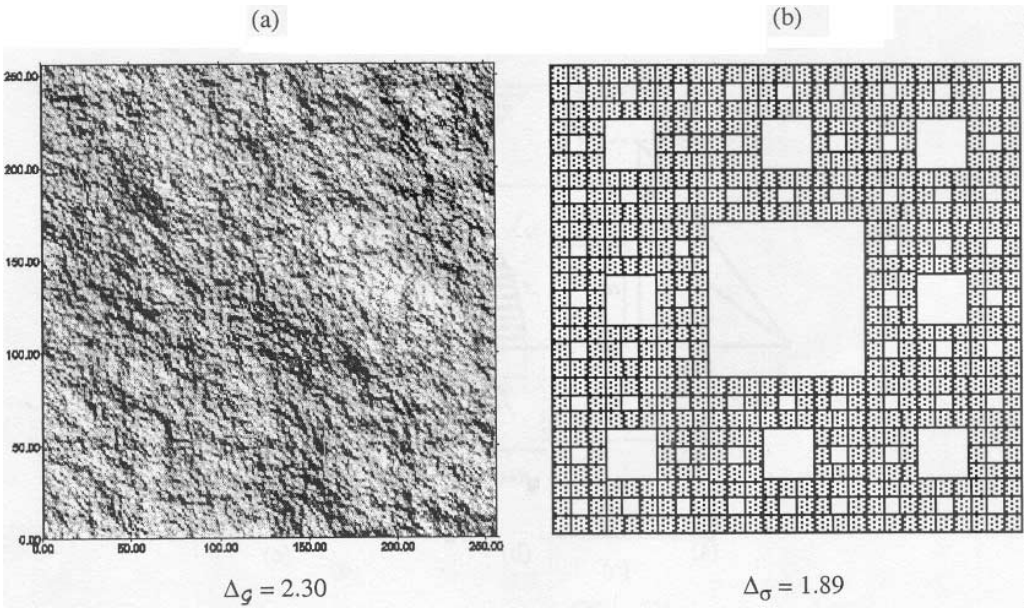

Figure 6. Invasive fracture surface and lacunar stress-carrying ligament.

at the smallest scales. In particular, at the smallest scales, a Brownian disorder is the highest possible one (Carpinteri 1994b).

On the basis of these hypotheses, a Multifractal Scaling Law (MFSL) for the apparent tensile strength was proposed by the authors (Carpinteri *et al* 1995a).

$$\sigma_u(b) = f_t\,[1 + (1_{ch}/b)]^{1/2}\,. \tag{11}$$

This scaling law, shown in figure 8a, is a two-parameter model, where the asymptotic value of the nominal strength f_t, corresponding to the lowest nominal tensile strength, is reached only in the limit of infinite sizes. The dimensionless term into square brackets, which is controlled by the characteristic length value l_{ch}, represents the variable influence of disorder on the mechanical behaviour, thus quantifying the difference between the nominal quantity measured at the scale b and the asymptotic characteristic value. In the bilog-

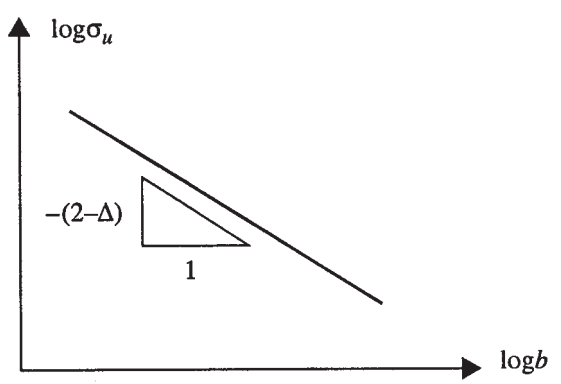

Figure 7. Monofractal size effect law.

arithmic diagram, shown in figure 8b, the transition from the fractal regime to the homogeneous one becomes evident. The threshold of this transition is meaningfully represented by point Q, whose abscissa is equal to $\log l_{ch}$. The oblique asymptotic is controlled by a quantity with the dimensions of a stress-intensity factor ($[F][L]^{-3/2}$), signifying that LEFM comes into play only when the characteristic size a of micro defects is comparable with the external size (highest disorder), whereas, at larger scales, the correlation among the microcracks increases, leading to the homogenization in the limit of infinite size (ordered regime).

It is worth pointing out here that l_{ch} is a quantity related to the material microstructural characteristics, but also depends on the loading geometry and on the choice of the reference size b. As a first approximation, the characteristic length l_{ch} can be related to some peculiar component of the concrete microstructure, e.g. to the maximum aggregate size $d_{\max}$. This length parameter is important when the scaling behaviour of two different materials is compared, as shown in figure 9. It can be stated that, in the case of a finer grained material like a high-strength concrete (HSC), the MFSL is shifted to the left with respect to the case of ordinary concrete (NSC), the value of the internal length being much lower for HSC than for NSC. Therefore, two specimens of different materials, with the same structural size b_1, besides obviously showing two different values of the nominal tensile strength, have to be set in two different scaling regimes.

With reference to figure 9, the normal concrete specimen behaves accordingly to the fractal regime, whereas the HSC one lies on the asymptotic branch of the MFSL, thus showing homogeneous macroscopic behaviour. It is interesting to note the faster transition to homogeneous scaling occurring in the case of HSC. This corresponds to the well-known brittle structural behaviour of plain high-strength concrete structures, where the comparatively large strength values are counterbalanced by smaller toughness values with respect to ordinary concrete structures. Generally speaking, one has to determine for each material the proper range of scales where the fractal regime is predominant, and consequently the minimum structural size beyond which the local mechanical fluctuations are macroscopically averaged and a constant value of the strength can be determined.

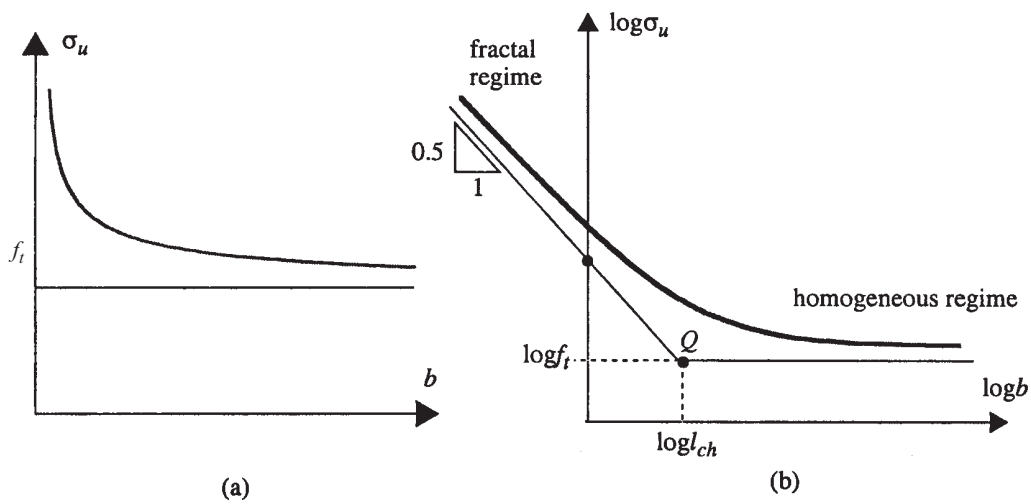

Figure 8. Multifractal scaling law for ultimate strength.

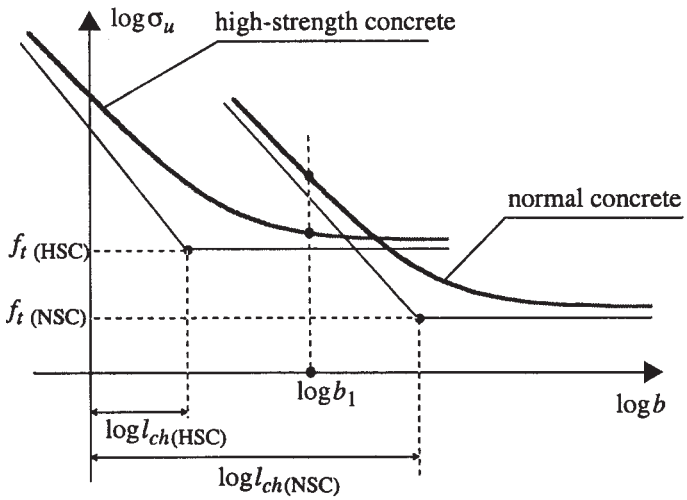

Figure 9. The MFSL applied to two different concretes.

4. Application to unnotched structures

As already pointed out in the previous sections, several experimental results indicate that even the largest members without initial crack possess an intrinsic strength, contrarily to the SEL predictions. Therefore, based on the experimental evidence, wide statistical investigation has been carried out by the authors on the size-effect data available in the literature (Carpinteri *et al* 1995b). Many testing geometries have been considered, either with unnotched or with notched specimens. In this section, some of the most significant tests on unnotched specimens are described. In the next section, attention will be drawn to notched specimens, and the basic differences between the two cases will be discussed. The nominal strength at failure will be hereinafter called σ_u (or τ_u, in the case of prevailing shear), regardless of the testing geometry.

The first geometry that will be discussed is a three-point bending test campaign performed at the Politecnico di Torino (Bosco *et al* 1990) on high strength concrete specimens. The beams used in this experimental investigation were made of concrete with crushed aggregate of maximum size $d_{\max} = 12.7$ mm. The amount of cement was 4.8 kN/m^3, and the water/cement ratio was equal to 0.27. The average compressive strength (after 28 days), obtained from 20 cubic specimens, was $f_c = 91.2$ N/mm^2. The elastic modulus was determined by testing three specimens measuring $150 \times 150 \times 450$ mm. An average value of the secant modulus E equal to 34300 N/mm^2 was obtained. The fracture energy $\mathcal{G}_F$ was determined according to the recommendation of the RILEM (1985). The average value was $\mathcal{G}_F = 0.090$ N/mm, so that the critical value of the stress-intensity factor could be evaluated as $K_{IC} = (\mathcal{G}_F E)^{-1/2} = 55.56$ N/mm$^{-3/2}$.

Thirty reinforced concrete beams were tested, with constant cross-section thickness $t = 150$ mm and depths $b = 100$, 200 and 400 mm, respectively. The span L between the supports was assumed to be equal to six times the beam depth $b(L = 600, 1200$ and2400 mm, respectively). Thus, only a two-dimensional similitude was present. The content of steel depended on the beam size and on the brittleness number $N_P = (f_{ys} b^{1/2} A_s)/(K_{IC} A_c)$ (Carpinteri 1986). Four different values of brittleness number, corresponding to four different collapse mechanisms, were adopted. Here, results are presented for beams with $NP = 0.53$. For these beams, the steel bars had nominal diameters ϕ equal to 4, 5, 8 and 10 mm respectively. The distance of the bars from the lower beam edge was, in each case, equal to one tenth of

the total beam depth b. No shear reinforcement was present. All the beams were initially unnotched.

The three-point bending tests were performed by a servo-controlled machine. The beams were supported by a cylindrical roller and a spherical connection at the two extremities. The load was applied through an hydraulic actuator, and the loading process was displacement-controlled by a strain-gauge, placed on the lower beam edge, parallel to the beam axis and symmetrical with respect to the force. Its length was equal to the beam depth.

The nominal stress at failure used for the statistical analysis can be set, according to the elastic bending theory, equal to:

$$\sigma_u(b) = 6M_u/tb^2, \tag{12}$$

where M_u is the failure bending moment. The test results (average values) are plotted as data points in a $\log \sigma_u$ versus $\log b$ diagram (figure 10a). The data are fitted by the MFSL in the form of (11). In this way, the best-fit parameters f_t (asymptotic strength valid for large-sized beams) and l_{ch} (characteristic length governing the transition from the region of strong size effect to the large sizes with constant strength) are provided. In this case, their values are determined as $f_t = 5.65$ MPa and $l_{ch} = 102.12$ mm. The dimensionless ratio between l_{ch} and the maximum aggregate size is equal to 8.04.

Afterwards, data can be fit by bažant's Size Effect Law, (2). While the correlation coefficient R (computed from the mean values) is equal to 0.974 in the case of the MFSL fitting, it is only equal to 0.883 in the case of the SEL fitting. Thus, the MFSL provides a better fit of test data. Graphically, it is evident that the data in the log-log plot suggest a curvature opposite to that of the SEL and that the decrement of the nominal strength tends to attenuate by increasing the structural size b. This means that, as $b \to \infty$, the nominal strength attains an asymptotic finite value, as predicted by the MFSL.

Four-point bending tests were carried out by Sabnis & Mirza (1979) on unnotched plain concrete specimens in the size range 1:17. The span to depth ratio was set equal to 4 for all the beams. As in the case of three-point bending, the nominal bending strength can be defined, according to (12), as the elastic stress acting upon the extreme fibre under failure load. Best-fit of the experimental data is shown in figure 10b. The asymptotic bending strength f_t, valid for the largest beams, is found to be equal to 3.83 MPa, whereas the characteristic length is $l_{ch} = 42.02$ mm. The correlation coefficient R is equal to 0.999 in the case of MFSL and to 0.952 in the case of SEL, being the concavity of the data which is clearly upwards in the bilogarithmic diagram.

Another series of four-point bending tests was carried out by bažant & Kazemi (1991) on unnotched reinforced concrete beams. Only longitudinal steel bars were present in the beams. The examined size range was 1:16 ($b = 20.64 \div 330.2$ mm), and a two-dimensional similitude was ensured, the thickness t being constant for all the beams ($t = 38.1$ mm). A micro-concrete was used, with maximum aggregate size $d_{\max}$ equal to 4.8 mm and average compressive strength $f_t = 46.2$ MPa. The span/depth ratio was set equal to 7. Therefore, even if diagonal shear failure was forced by the presence of the bars, flexural effects cannot be excluded *a priori*. The steel bars, anchored with right-angled hooks at their ends to prevent bond slip and pull-out, provided a reinforcement ratio $\rho = A_s/A_c = 1.62\%$.

According to the assumed diagonal shear collapse, the nominal strength can be set equal to the nominal shear strength, that is:

$$\tau_u = P_u/2bt, \tag{13}$$

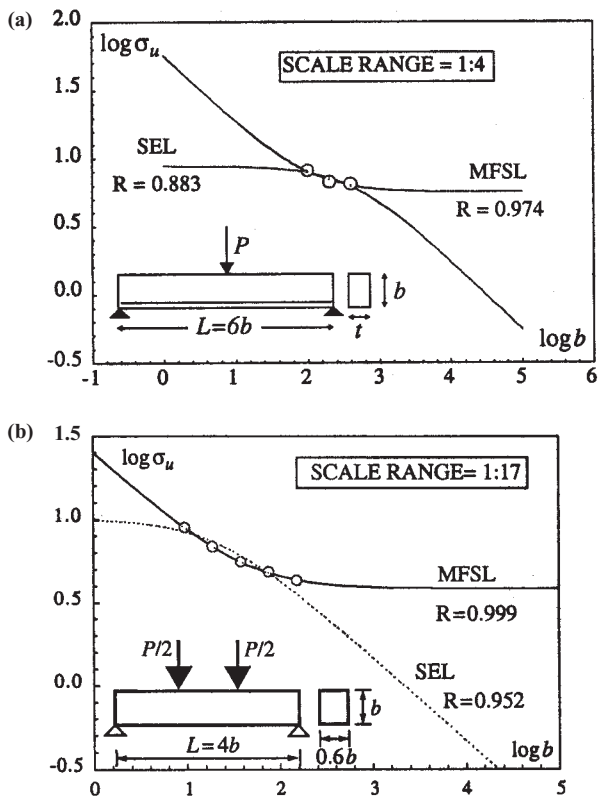

Figure 10. Fitting the data by Bosco *et al* (1990) **(a)**, and the data by Sabnis & Mirza (1979) **(b)**.

where P_u is the failure load. Best-fit of the data by means of MFSL yields the following parameters: $f_t = 0.571$ MPa and $l_{ch} = 485.9$ mm, with a correlation coefficient R equal to 0.986 Instead, fitting the data by SEL yields the value $R = 0.980$ (figure 11). If the characteristic length is supposed to be directly proportional to $d_{\max}$, a nondimensional ratio can be found equal to $\alpha = l_{ch}/d_{\max} = 101.23$.

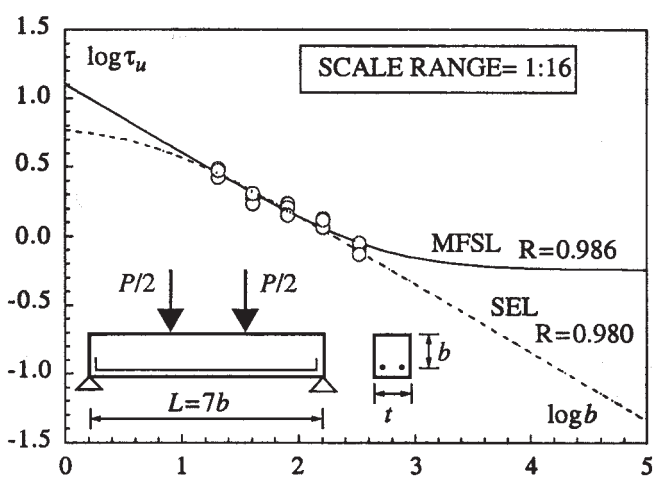

Figure 11. Fitting the data by Bažant & Kazemi (1991).

Another interesting test geometry is represented by the *splitting cylinder tests* carried out by Hasegawa *et al* (1985). Concrete cylinders, geometrically similar in two dimensions (the height h of the cylinders is constant and equal to 500 mm), have been tested in the wide size range 1:30 ($b_{\min} = 100$ mm, $b_{\max} = 3000$ mm). The maximum aggregate size was equal to 25 mm, whereas the average compressive strength was equal to 23.4 MPa. The nominal tensile strength is supposed to be equal to the maximum principal stress, according to the theory of elasticity:

$$\sigma_u(b) = 2P_u/\pi bh, \tag{14}$$

where P_u is the ultimate load, and b and h are respectively the diameter and the (constant) height of the cylinder specimens.

Application of the MFSL is plotted in the bilogarithmic diagram (figure 12), where best-fit by Bažant's SEL is also shown for comparison. The computed best-fit values are $f_t = 1.45$ MPa and $l_{ch} = 199.2$ mm. Note that the asymptotic strength f_t is equal to 80% of the average of the ultimate tensile stresses (1.80 MPa) and only to 56% of the smallest specimens' strength. The parameter $\alpha = l_{ch}/d_{\max}$ is equal to 7.96. The correlation coefficient yielded by the MFSL is $R = 0.966$, whereas Bažant's SEL yields R = 0.663. Note that, in the case of tests characterized by wide size ranges, MFSL reproduces the scaling behaviour of tensile strength, much better than SEL, the concavity of data being clearly upwards according to the aforementioned transition to the homogeneous regime.

Pull-out tests have been performed by Eligehausen *et al* (1992) and by Bažant & Sener (1988). The first series consists in the extraction of anchor steel bolts from similar prismatic concrete specimens, with the dimensional ratio 1:3:9 (b = bar embedment depth = 50, 150 and 450 mm). Three-dimensional similitude is ensured by proper scaling of all the sizes of the specimens. All the specimens have been cast from the same batch of concrete, characterized by an average compressive strength equal to 30 MPa and by the maximum aggregate size equal to 22 mm.

In all the specimens, a tensile failure mechanism was detected, consisting in the removal of a concrete cone with height equal to the depth of the steel bar (figure 13a). The nominal stress at failure, computed from the ultimate load P_u, is defined according to:

$$\sigma_u(b) = \frac{P_u}{A_{cone}} = \frac{P_u}{(\pi 3b^2)/4}. \tag{15}$$

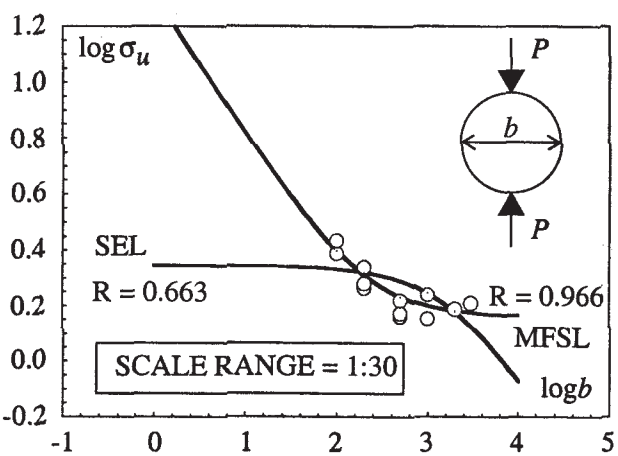

Figure 12. Fitting the data by Hasegawa *et al* (1985).

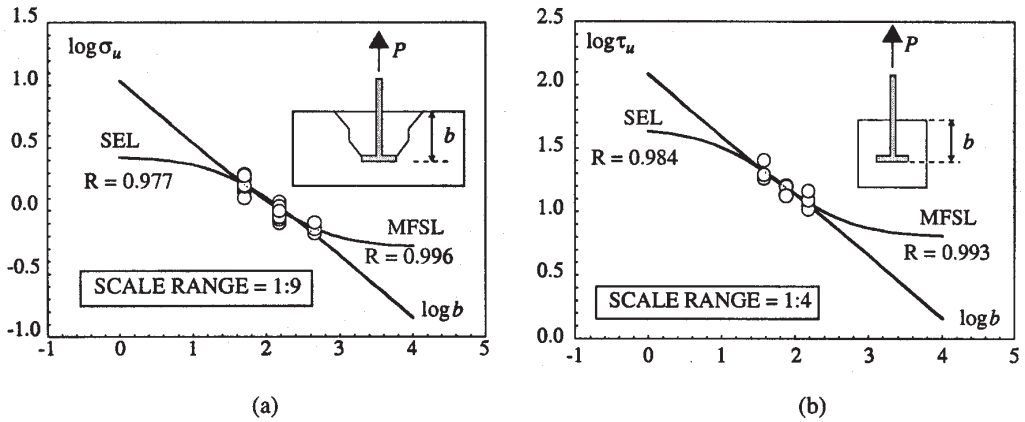

Figure 13. Fitting the data by Eligehausen *et al* (1992) **(a)**, and the data by Bažant & Sener (1988) **(b)**.

The application of MFSL and SEL to the experimental data is shown in figure 13a. The strength values have been normalized to the average compressive strength. The best-fit values are $f_t = 0.518$ MPa and $l_{ch} = 438.6$ mm, yielding $\alpha = l_{ch}/d_{\max} = 19.9$. Fitting by the MFSL provides $R = 0.996$, whereas fitting by the SEL gives $R = 0.977$. In this case, also due to the limited size range tested, data could be adequately fitted by a straight line (monofractality).

The pull-out tests by Bažant & Sener (1988) confirm the slight upward concavity in the bilogarithmic diagram. Anyway, in this case, the size range (1:4) is too small to ensure sufficient statistical reliability. Cubic micro-concrete ($d_{\max} = 6.4$ mm) specimens have been tested, with average compressive strength f_c equal to 45.8 MPa. A three-dimensional similarity is ensured among the specimens. The collapse mechanism was totally different from the cone failure detected by Eligehausen *et al* (1992) because, in this case, the contrast plates act close to the steel bar. Failure occurred either by slipping of the bar or by splitting of the surrounding concrete, caused by the strong radial tractions originating from the bar. A conventional strength can be defined according to:

$$\tau_u(b) = \frac{P_u}{A_{adherence}} = \frac{P_u}{(\pi d_{bar})b}, \tag{16}$$

being d_{bar} and b respectively the diameter and the embedment depth of the bar. The application of MFSL and SEL to the experimental data is shown in figure 13b. In this case the strength values have not been normalized. The best-fit procedure yields $f_t = 6.4$ MPa, $l_{ch} = 362.5$ mm and $\alpha = l_{ch}/d_{\max} = 56.6$. Best-fit by MFSL provides $R = 0.993$, whereas application of the SEL gives $R = 0.984$. Note that, also in this case, the linear (monofractal) approximation of the scaling laws is satisfactorily reliable, due to the narrow range of sizes that has been considered.

Many other test geometries have been investigated by means of MFSL and SEL (Carpinteri *et al* 1995b). The upward curvature in the log-log plot has been detected in almost all cases (see, for instance, the uniaxial tensile tests by Carpinteri & Ferro (1994) or the torsional tests by Barr & Tokatly 1991). Only rare exceptions have been found, one being represented by the double-punch tests carried out by Marti (1989) where a downward curvature was detected in the log-log plot. In conclusion, it seems that, in the case of unnotched specimens, energy

release effects assume a leading role in the definition of strength only when the crack formed before maximum load is large compared to the dimension of the structure, that is, when the (unnotched) structure is sufficiently small. Thereby, the transition from the fractal regime to the homogeneous one prevails, and size effects are interpreted by the MFSL consistently.

5. Application to notched structures

In this section, some experimental results obtained by tests on notched specimens are discussed. It should be pointed out that, although in this case a more controlled failure behaviour can be ensured, concrete structures with macro-notches scaling proportionally to their size are far from engineering practice.

The first tests to be considered are the uniaxial tensile tests performed by Bažant & Pfeiffer (1987). Prismatic specimens have been tested, where the rectangular cross-sections had constant thickness $t = 19$ mm and span/height ratio equal to 8/3. The cross-section heights of the specimens were $b = 38.1$, 76.2 and 152.4 mm. Thus, a narrow scale range (1:4) was investigated. Two symmetrical notches were cut by a diamond saw at midspan, with depth a equal to $b/6$ and thickness t equal to 2.5 mm. Therefore, as required by bažant's SEL, the notches scaled proportionally to the specimens' linear size. The concrete mixture was made with a water/cement ratio of 0.6 and a maximum aggregate size $d_{\max} = 12.7$ mm. The mean compressive strength after 28 days curing was $f_c = 33.5$ MPa. The special loading grip designed for these specimens was made by two aluminum plates bolted together. According to the classical theory, the nominal strength can be defined as the stress acting upon the net section at maximum load:

$$\sigma_u = P_u / [t(b - 2a)], \tag{17}$$

where P_u is the maximum tensile load and $t(b - 2a)$ is the net cross-section. Fitting the experimental data by MFSL yields $f_t = 2.82$ MPa and $l_{ch} = 29.2$ mm, with $\alpha = l_{ch}/d_{\max} = 2.30$. The correlation coefficient obtained by the MFSL is $R = 0.952$, while the SEL provides a better fit, with $R = 0.998$ (figure 14a).

Another series of uniaxial tensile tests on notched concrete specimens was carried out by Nooru-Mohamed & Van Mier (1991). Prismatic specimens were tested, with dimensions (span × height × thickness) equal to 200 × 200 × 50, 100 × 100 × 50 and 50 × 50 × 50 mm. Thus, only a narrow scale range (1:4) was investigated. Tests were carried out under displacement control by four LVDTs mounted very close to the notches. Two symmetrical notches were cut at midsize of the specimens. As in the tests by Bažant & Pfeiffer (1987), the notch depth a scaled proportionally to the specimen's height b by setting, in each specimen, $a/b = 0.125$. A micro-concrete (with water/cement ratio equal to 0.5 and mean compressive strength $f_c = 49.7$ MPa) was used, with $d_{\max} = 2$ mm. The nominal tensile strength can be defined again as the stress acting upon the net section at maximum load (17). Fitting the data by MFSL yields $f_t = 0.96$ MPa and $l_{ch} = 44.8$ mm, with $\alpha = l_{ch}/d_{\max} = 22.4$. The correlation coefficient obtained by the MFSL is $R = 0.917$, while the SEL provides a better fit, with $R = 0.988$ (see figure 14b).

Three-point bending tests on notched plain concrete beams were carried out by Perdikaris & Romeo (1992). Two mixtures of concrete were examined, with the same granularity ($d_{\max} = 6.4$ mm), but with different compressive strengths. In the case of the first series, f_c(I) was equal to 35 MPa whereas, in the case of series II, higher strength was obtained (f_c(II) = 75.5 MPa). The examined size range was equal to 1:4 for both the series and only a two-dimensional

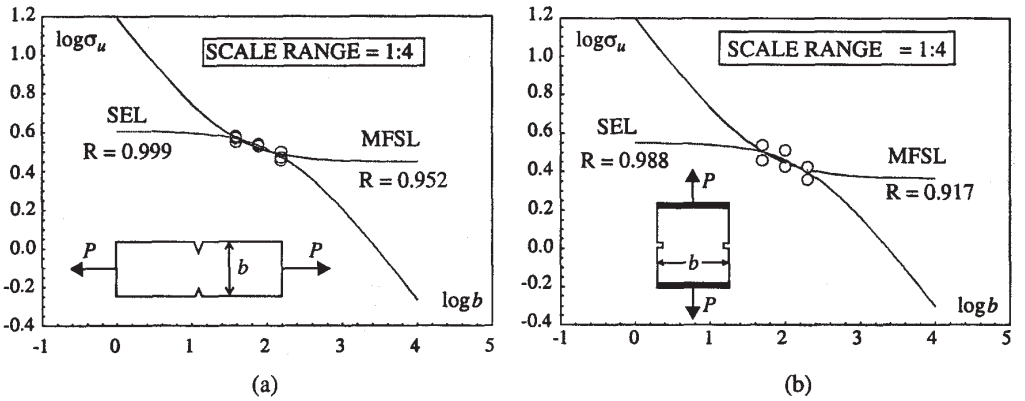

Figure 14. Fitting the data by Bažant & Pfeiffer (1987) **(a)**, and the data by Nooru–Mohamed & Van Mier (1991) **(b)**.

similitude was present, being $L = 4b$ and the thickness t of the beams constant and equal to 127 mm. A nominal strength σ_u can be defined, according to the elastic bending theory, equal to:

$$\sigma_u = 6M_u / \left[t(b - a_0)^2\right], \tag{18}$$

where M_u is the bending moment at failure, t and b are respectively the beam thickness and depth, and $a_0 = 0.3b$ is the initial notch length. The application of the MFSL to the nominal strength data from series I (normal-strength concrete, NSC) is described in figure 15a. The best-fit values are respectively $f_t = 1.41$ MPa and $l_{ch} = 562.8$ mm, with the nondimensional parameter α equal to 87.9. The correlation coefficient determined by MFSL results in $R = 0.980$, whereas fitting by SEL provides $R = 0.991$. The application of the MFSL to the data from series II (high-strength concrete, HSC) is shown in figure 15b. In this case, best-fit provides $f_t = 4.21$ MPa, $l_{ch} = 131.1$ mm, $\alpha = 20.5$ and $R = 0.901$. SEL provides a better goodness of fit in this case also, being $R = 0.965$. Note that, according to the MFSL arguments, l_{ch} (HSC) $< l_{ch}$ (NSC).

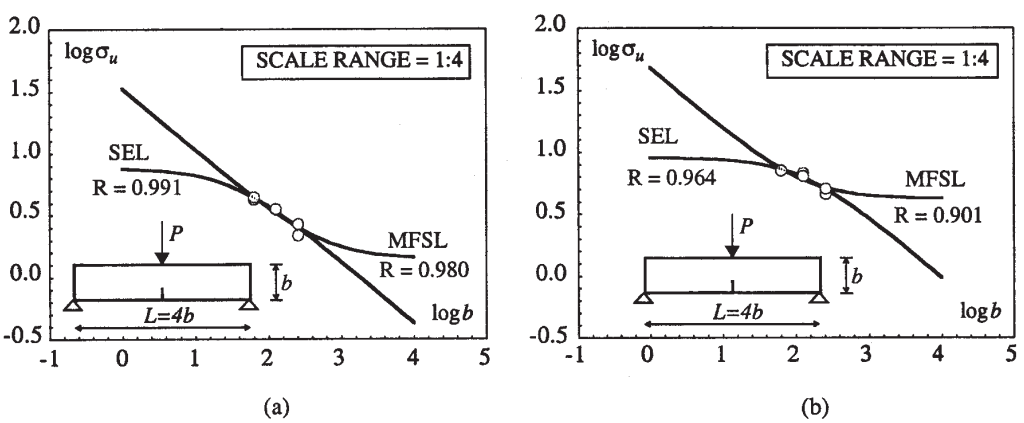

Figure 15. Fitting data by Perdikaris & Romeo (1992).

An interesting comparison can be made between the strength and toughness properties of the two series. While, in fact, the compressive strength value of series II is 114% larger than in the case of series I, and the asymptotic (nominal) tensile strength of series II is almost 300% larger than in the case of series I, a much smaller difference (24%) between the asymptotic fracture energies of the two series has been detected. This confirms the (relative) increase of brittleness corresponding to the increase of compactness and homogeneity in the microstructure which, in its turn, aims to increase the strength value. The transition to more brittle behaviour, in the case of the HSC, can be synthesised by means of the brittleness number $s = \mathcal{G}_F/\sigma_u b$. Setting, for instance, $b = 100$ mm for both series, one obtains $S_{(\text{Series I})} = 0.00091$ and $S_{(\text{Series II})} = 0.00038$, thus concluding that the larger the strength, the larger the brittleness.

Another three point bending campaign was carried out, by Gettu *et al* (1990), on notched *high strength concrete* beams, with average compressive strength equal to 96 MPa. This kind of material, where silica fume and fly ash are also present, is characterized by relatively small aggregates and by a strong bond between matrix and aggregates. The strength of the cementitious matrix is comparable with that of the aggregates, thus resulting in a *more homogeneous* fracture process with respect to ordinary concrete. In fact, the width of the fracture process zone, according to the cohesive model, decreases almost by 60%. Consequently, while the compressive strength increases almost by 160%, the material's fracture energy increases only by 25%, resulting in the *brittleness number* thus being halved. This provides definitely more brittle behaviour with respect to ordinary concrete, implying, in the multifractal scaling law, rapid transition towards an ordered regime, characterized by the absence (or, better, by the homogenization) of the positive contribution to microstructural disorder.

Four similar prismatic specimens were tested, all notched at midspan and subjected to bending. The reference structural size b was chosen equal to the total beam depth (considering also the notch), that is, equal to 38.1, 76.2, 152.4 and 304.8 mm respectively (range 1:8). The notch depth a_0, scaled in a proportional manner with b, was set equal to $b/3$, while the net span between the supports was $L = 2.5b$. Note that only a two-dimensional similitude was provided, being the thickness t of all the specimens, constant and equal to 38.1 mm. The maximum aggregate size was 9.5 mm. Nominal tensile strength can be computed according to the theory of elasticity, assuming the initially uncracked ligament (see (18)) as the resistant section.

Fitting the data by the MFSL provides $f_t = 4.1$ MPa and $l_{ch} = 156.9$ mm, with $\alpha = l_{ch}/d_{\max} = 16.51$. The MFSL correlation coefficient is $R = 0.981$, whereas the application of SEL yields $R = 0.914$ (figure 16). It can be argued that the strength values obtained from the largest specimens are too large, because they are in clear disagreement with the SEL predictions. On the contrary, these values show perfect agreement with the MFSL, as they are placed in the asymptotic homogeneous regime of the scaling, which, in the case of high strength concrete, comes into play much earlier. Note also that the asymptotic strength f_t is equal to 60% of the specimens' average strength ($\overline{\sigma}_m = 6.8$ MPa), and only to 43% of the smallest specimens' one.

In conclusion, the downward curvature in the log-log plot has been detected mostly in cases where initially notched structures have been considered, with their notches scaling proportionally to the structure size (Carpinteri *et al* 1995b). It seems that, in these cases, energy release effects are prominent and thus the size effect law according to bažant is an appropriate scaling model. However, some exceptions are present, like the three-point bending tests by Gettu *et al* (1990) where the MFSL is more adherent to the experimental data. Moreover, the

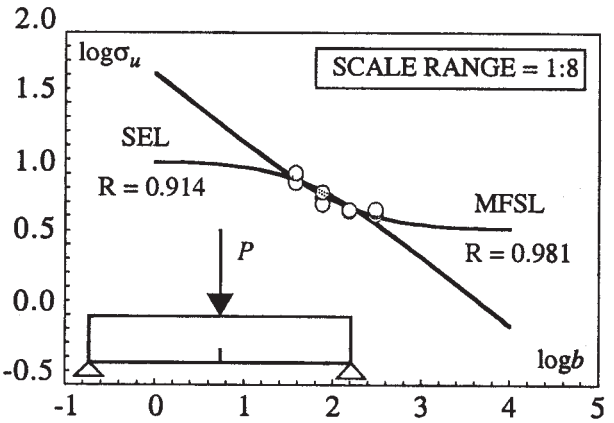

Figure 16. Fitting the data by Gettu *et al* (1990).

engineering significance of tests where the initial notch can be larger than a few centimetres, is questionable. Unfortunately, the size range considered in the tests is often too narrow to draw final conclusions. The need for large-scale testing is nowadays widely diffused in concrete engineering, and only experiments on large structures can give the final validation to the theories.

6. Conclusions

6.1 *Engineering considerations*

Despite the need for large-scale testing, the major advantage of the MFSL is that it allows for the determination of the finite asymptotic strength of very large concrete structures. On the contrary, Bažant's SEL would uselessly predict zero strength for large elements. A wide number of experimental tests confirm the MFSL hypotheses. Size-dependence is found to be stronger in the range of smaller sizes, as well as the scatter of the strength values corresponding to a certain size is smaller for the largest sizes. This clearly indicates that heterogeneity plays a fundamental role. Recent experimental results by Adachi *et al* (1995) demonstrate that the same transition is present also in the scaling of the deformability characteristics of concrete beams subjected to bending. The negative size-effect on the maximum rotational capacity turns out to be, in fact, more pronounced as the depth of the beams becomes shallower.

In order to apply the MFSL to real engineering cases, it is worth discussing the definition of the reference size b to be considered in the scaling law. If a perfect three-dimensional similitude were present *with respect to the failure mechanism*, any linear size of the structure could be used. But this is seldom the case, and thus one should determine, in each case, the opportune definition of b. For instance, given two structures to compare, one should determine the representative region (this being an area or a volume) where similar stress–strain conditions are present and failure is more likely to occur. In the case of bending, for example, the height b at midspan of the beam would be the representative size only if the beam span L and the beam thickness t were both scaled proportional to b (3D similitude). If this were not the case, for instance, if the thickness t were constant, it would be more correct to adopt the value as the reference size $b^* = \sqrt{bt}$. Analogously, in the case of two cooling towers, one should compare the circular strips where failure is expected to originate caused by tensile membrane stresses (figure 17). The thickness t of the membrane should be adopted

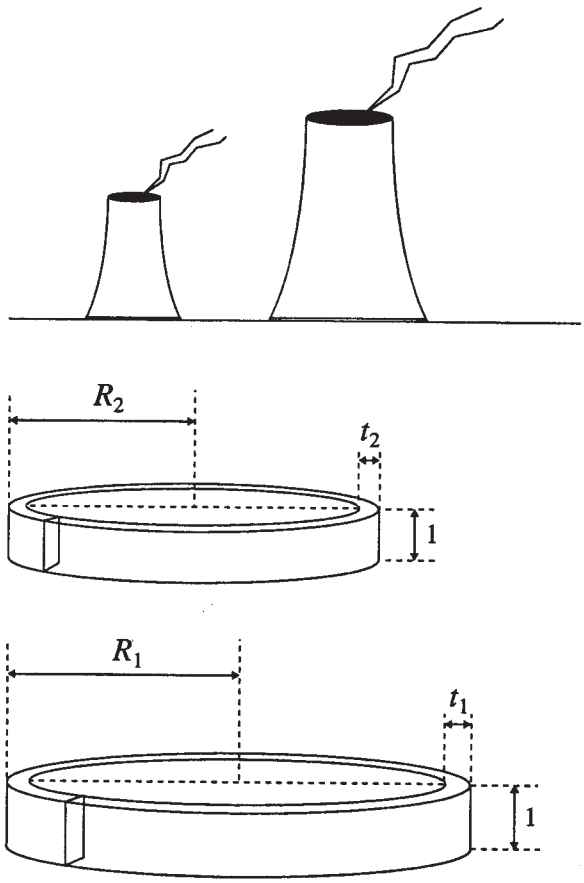

Figure 17. Structural similitude for concrete cooling towers.

as the reference size only if the radius (and the tower height) were scaled proportionally. Otherwise, it could be more correct to use the value $b^* = \sqrt{Rt}$ as the reference size.

6.2 *Final remarks*

On the basis of theoretical and experimental evidence, the following conclusions may be drawn:

(1) The current building-code requirements need to be revised, if consistent and reliable predictions are to be made for the strength of real-sized concrete structures. Poor extrapolations from laboratory-sized specimens are obtained, if the size-dependence of the ultimate strength is not properly taken into account. Moreover, existing formulas (CEB-FIP 1991; ACI 1992; CEC 1994) are based on an empirical approach which cannot be considered suitable for the huge variety of material properties and structural types that are nowadays encountered.

(2) The need for correct prediction of the bending strength of concrete beams is neither restricted to unreinforced elements nor confined to the durability requirements of the reinforced ones, but rather plays a fundamental role in the definition of the minimum reinforcement ratio and of the failure characteristics of the largest members. The determination of reliable values of the modulus of rupture seems to be even more important in

the case of high-strength concrete, where more brittle behaviour is expected and bending failure may be catastrophic.

(3) The heterogeneity of the concrete microstructure is strongly responsible for the size-dependence of strength. Therefore, mechanical arguments have to be supported by an adequate topological description of the failure process, for which fractal geometry seems to represent a powerful and successful tool. The interplay between microstructural characteristic length and external size of the beam implies progressive vanishing of disorder effects on the strength characteristics, which can be adequately modelled by means of a multifractal scaling transition. The same transition also seems to affect the deformability properties, namely the maximum rotational capacity of concrete beams in bending.

(4) Multifractal scaling law has been put forward by the authors, which allows for the extrapolation of a reliable value of the ultimate strength holding for real-sized structural members. The validity of the MFSL has been confirmed by statistical investigation over a multitude of experimental data reported in the literature. On the other hand, wider ranges of sizes should be tested in order to get better statistical reliability.

(5) The very general physical arguments underlying the aforementioned approach seem to claim its applicability not only in the case of purely tensile and bending failures but also in the case of shear failures, where aggregate interlock and mixed mode cracking are affected by microstructural heterogeneities.

(6) Regarding the long-time controversy with Z P Bažant, it is worth pointing out that invasive fractals, i.e. fractal sets with scale-densifying topological properties (see §3.1), have never been put forward to justify strength size-effects, as erroneously reported by Bažant (1997). The invasive fractals, on the other hand, are useful for explaining the (positive) size-effect on fracture energy (Carpinteri & Chiaia 1995). In addition, the lacunar fractality assumption is regarding the material ligament (or the net cross-section), and not the microcracks array, as Bažant (1997) probably misunderstood.

(7) Moreover, Bažant (1997) properly affirms that the energy release due to fracture increases with the structure size faster than the energy dissipated by the fracture. This is nothing but the very well-known Griffith's energy approach which produces a strength decrease with slope equal to $-1/2$ in the $\log \sigma_u - \log b$ plot. The size effect caused by the release of energy from the structure is taken into account in the MFSL exactly when, as Bažant notes, the crack formed before maximum load is large compared to the size of the structure, i.e. when the (unnotched) structure is sufficiently small. When the structure is larger, the crack formed before maximum load could be very small, or even absent when a very brittle (catastrophic) failure occurs. On the other hand, a homogenization effect should prevail in the case of very large specimen sizes, due to the limited size of the heterogeneities (aggregates, pores, cracks etc.). The two-limit situations of small scales (slow crack growth and geometric disorder) and large scales (fast crack propagation and geometric order), must be connected by an envelope curve with decreasing slope in the log-log plot (from $-1/2$ to zero). The MFSL derived from the above arguments presents a characteristic internal length, as expected by Bažant (1997).

(8) Several of the test data reported in the literature could be equally well fitted by the size effect law (Bažant 1984), but only when the scale range is below one order of magnitude. In the other few cases, a finite asymptotic value of nominal strength emerges for large-sized (unnotched) specimens, exhibiting an upward curvature in the log-log plot. This is nothing but the homogenization effect mentioned above.

(9) As a last remark, we willingly admit that the size effect law according to bažant is appropriate when initially cracked or notched structures are considered, with their cracks or notches scaling proportionally to the structure size. On the other hand, when the structures are initially uncracked and unnotched, this law is not appropriate and must be generalized to consider the homogenization effects, in the framework of self-affine geometry.

The authors gratefully acknowledge financial support by the Ministry of University and Scientific Research (MURST), by the Italian Research Council (CNR) and by the EC-TMR Contract N° ERBFMRXCT 960062.

References

Adachi H, Shirai N, Nakanishi M, Ogino K 1995 Size effect on strength and deformation of RC beams failing in flexure. In *Proce. 2nd Int. Conf. on Fracture Mechanics of Concrete Structures (FRAMCOS-2)* (ed.) F H Wittmann (Freiburg: Aedificatio Publ.) pp 685–692

ACI 1992 *American Concrete Institute: Building Code 318R-89* (Detroit: ACI Press)

Bažant Z P 1984 Size effect in blunt fracture: concrete, rock, metal. *J. Eng. Mech., Am. Soc. Civil Eng.* 110: 518–535

Bažant Z P 1997 Scaling of quasibrittle fracture: hypotheses of invasive and lacunar fractality, their critique and Weibull connection. *Int. J. Fracture* 83: 41–65

Bažant Z P, Chen E P 1997 Scaling of structural failure. *Appl. Mech. Rev.* 50: 593–627

Bažant Z P, Kazemi M T 1991 Size effect on diagonal shear failure of beams without stirrups. *ACI Struct. J.* 88: 268–276

Bažant Z P, Li Z 1995 Modulus of rupture: size effect due to fracture initiation in boundary layer. *J. Struct. Eng., Am. Soc. Civil Eng.* 121: 739–746

Bažant Z P, Pfeiffer P A 1987 Determination of fracture energy from size effect and brittleness number. *ACI Mater. J.* 84: 463–480

Bažant Z P, Sener S 1988 Size effect in pullout tests. *ACI Mater. J.* 85: 347–351

Barr B, Tokatly Z Y 1991 Size effects in two compact test specimen geometries. In *Applications of fracture mechanics to reinforced concrete* (ed.) A. Carpinteri: (London: Elsevier) pp 63–93

Bosco C, Carpinteri A, Debernardi P 1990 Minimum reinforcement in high-strength concrete. *J. Struct. Eng., Am. Soc. Civil Eng.* 116: 427–437

Brühwiler E, Broz J J, Saouma V E 1991 Fracture model evaluation of dam concrete. *J. Mater. Civ. Eng. Am. Soc. Civil Eng.* 3: 235–251

Carpinteri A 1986 *Mechanical damage and crack growth in concrete: Plastic collapse to brittle fracture* (Dordrecht: Martinus Nijhoff)

Carpinteri A 1989 Decrease of apparent tensile and bending strength with specimen size: two different explanations based on fracture mechanics. *Int. J. Solids Struct.* 25: 407–429

Carpinteri A 1994a Fractal nature of material microstructure and size effects on apparent mechanical properties. *Mech. Mater.* 18: 89–101

Carpinteri A 1994b Scaling laws and renormalization groups for strength and toughness of disordered materials. *Int. J. Solids Struct.* 31: 291–302

Carpinteri A, Ferro G 1994 Size effects on tensile fracture properties: a unified explanation based on disorder and fractality of concrete microstructure. *Mater. Struct.* 27: 563–571

Carpinteri A, Chiaia B 1995 Multifractal nature of concrete fracture surfaces and size effects on nominal fracture energy. *Mater. Struct.* 28: 435–443

Carpinteri A, Chiaia B, Ferro G 1995a Size effects on nominal tensile strength of concrete structures: multifractality of material ligaments and dimensional transition from order to disorder. *Mater. Struct.* 28: 311–317

Carpinteri A, Chiaia B, Ferro G 1995b Multifractal scaling law: an extensive application to nominal strength size effect of concrete structures. Report 51, Torino: Dept. Struct. Eng. Politec. Turin

Carpinteri A, Chiaia B 1996 Power scaling laws and dimensional transitions in solid mechanics. *Chaos, Solit. Fractals* 7: 1343–1364

Carpinteri A, Chiaia B, Ferro G 1997 A new explanation for size effects on the flexural strength of concrete. *Mag. Concr. Res.* 49: 45–53

CEB-FIP 1991 Comite' Euro-International du Beton. *Model Code-90 for concrete* (Lausanne: Thomas Telford)

CEC 1994 Commission of the European Communities Eurocode No.2 - Design of Concrete Structures

D'Arcy T W 1917 *On growth and form* (Cambridge: University Press)

Eligehausen R, Bouska P, Cervenka V, Pukl R 1992 Size effect of the concrete cone failure load of anchor bolts. In *Proc. First Int. Conf. on Fracture Mechanics of Concrete Structures (FRAMCOS1)* (ed.) Z P Bažant (Breckenridge: Elsevier) pp 517–525

Freudenthal A M 1968 Statistical approach to brittle fracture. In *Fracture* (ed.) H Liebowitz (New York: Academic Press) pp 591–619

Galilei G 1638 *Dialogues concerning two new sciences* (English Transl.). (London: Dover)

Gettu R, Bažant Z P, Karr M E 1990 Fracture properties and brittleness of high-strength concrete. *ACI Mater. J.* 87: 608–618

Griffith A A 1921 The phenomenon of rupture and flow in solids. *Philos. Trans. R. Soc. London* A221: 163–198

Hasegawa T, Shioya T, Okada T 1985 Size effect on splitting tensile strength of concrete. In *Proc. 7th Conf. of the Japan Concrete Institute* (Tokyo: JCI Publ) pp 309–312

Heilmann H G 1976 Zugspannung und Dehnung in unbewehrten Betonquerschnitte bei exzentrischen Belastung. *Deutscher Ausschuss fur Stahlbeton*, p. 269

Hillerborg A, Modeer M, Petersson P E 1976 Analysis of crack formation and crack growth in concrete by means of fracture mechanics and finite elements. *Cement Concr. Res.* 6: 773–782

Irwin G R 1957 Analysis of stresses and strains near the end of a crack traversing a plate. *J. Appl. Mech.* 24: 361–364

Jenq Y, Shah S P 1985 Two parameter fracture model for concrete. *J. Eng. Mech., Am. Soc. Civil Eng.* 111: 1227–1241

Kim J K, Eo S H 1990 Size effect in concrete specimens with dissimilar initial cracks. *Mag. Concr. Res.* 42: 233–238

Marti P 1989 Size effect in double-punch tests on concrete cylinders. *ACI Mater. J.* 86: 597–601

Neville A M 1981 *Properties of concrete* (London: Pitman)

Nooru-Mohamed M B, Van Mier J G M 1991 Size effect in mixed mode fracture of concrete. In *Fracture Processes in Concrete, Rock and Ceramics* (eds) J G M Van Mier, J G Rots, A Bakker (Amsterdam: EFN Spon) pp 461–471

Perdikaris P C, Romeo A 1992 Effect of size and compressive strength on the fracture energy of plain concrete. In *Proc. First Int. Conf. on Fracture Mechanics of Concrete Structures (FRAMCOS1)*: (ed.) Z P Bažant (Breckenridge: Elsevier) pp 550–555

Planas J, Guinea G V, Elices M 1995 Rupture modulus and fracture properties of concrete. In *Proc. 2nd Int. Conf. on Fracture Mechanics of Concrete Structures (FRAMCOS-2)* (ed.) F H Wittmann (Freiburg: Aedificatio Publishers) pp 95–110

RILEM 1985 Technical Committee 50, Determination of the fracture energy of mortar and concrete by means of three-point bend tests on notched beams, Draft Recommendation. *Mater. Struct*. 18: 287–290

Sabnis G M, Mirza S M 1979 Size effect in model concretes? *J. Struct. Div., Am. Soc. Civil Eng.* 105: 1007–1020

Tang T, Shah S P, Ouyang C 1992 Fracture mechanics and size effect of concrete in tension. *J. Struct. Eng., Am. Soc. Civil Eng.* 118: 3169–3185

Uchida Y 1992 Application of fracture mechanics to size effect on flexural strength of concrete. *Concrete Library of JSCE*, n°20 (Tokyo: JSCE Publ)

Weibull W 1939 *A statistical theory for the strength of materials* (Stockholm: Swedish R. Inst. Eng. Res.)